VOL. 11, NO. 23, DECEMBER 2016 ISSN 1819-6608
ARPN Journal of Engineering and Applied Sciences

www.arpnjournals.com

COMPUTATIONAL MODELING OF DIESEL AND DUAL FUEL COMBUSTION USING CONVERGE CFD SOFTWARE

Wan Nurdiyana Wan Mansor[1] and Daniel B. Olsen[2]
[1]School of Ocean Engineering, Universiti Malaysia Terengganu, Malaysia
[2]School of Mechanical Engineering, Colorado State University, United States of America
E-Mail: nurdiyana@umt.edu.my

ABSTRACT

In this study, CONVERGE CFD software is utilized for modeling processes in an internal combustion engine. CONVERGE includes advanced numerical techniques and physical models describing processes of spray, turbulence and combustion, and the nonlinear interactions of such processes. The objective of modeling dual fuel combustion is to gain better understanding of the combustion behavior in dual fuel engines. This modeling is performed in conjunction with experimental studies on a John Deere 6068H diesel engine. The engine is a Tier II, 6 cylinders, 6.8 liter, 4-stroke compression ignition engine with a compression ratio of 17:1 and a power rating of 168 kW at 2200 rpm. A natural gas fuel system was installed to deliver fuel upstream of the turbocharger compressor. The engine was operated at 1800 rpm through two different load points in diesel and dual fuel operating modes. Motored pressure, combustion pressure and net heat release rate (HRR) generated from the simulations are compared to the corresponding experimental results. Additionally, temperature, equivalence ratio, carbon monoxides and total hydrocarbon emissions distributions in dual fuel simulations at 12% and 75% loads are presented and discussed.

Keywords: dual fuel engine, converge CFD, computational fluid dynamics.

INTRODUCTION

Recently, alternative fuels have been getting more attention as concerns escalate over exhaust pollutant emissions produced by internal combustion engines, higher fuel costs, and the depletion of crude oil. Many researchers have been searching for a way to overcome these issues while maintaining the standard internal combustion engine infrastructure [1]. Various solutions have been proposed, including utilizing alternative fuels as a dedicated fuel in spark ignited engines, diesel pilot ignition engines, gas turbines, and dual fuel engines. Among these applications, one of the most promising options is the diesel derivative dual fuel engine with natural gas as the primary fuel.

Natural gas, which is primarily composed of methane, is considered to be a viable alternative to liquid petroleum-based fuels. As a global resource natural gas is abundant. It is particularly well suited for dual fuel applications where it is introduced to high compression ratio engines due to high octane numbers and auto-ignition temperatures. In the diesel derivative dual fuel engine, a mixture of air and natural gas is inducted to the cylinder during the intake stroke. The mixture is then compressed and ignited when a diesel fuel jet is injected near top dead center. The dual fuel engine can be run with 100% diesel fuel or operate as a dual fuel engine with the availability of natural gas. The engine will not operate as a dedicated natural gas unit because an ignition source is required.

A number of experimental and theoretical research investigations have been published concerning the diesel/natural gas dual fuel engine. The focus has been on the variation in combustion due to the effects of diesel fuel quantity, injection timing, injector nozzle design, injection pressure and exhaust gas recirculation [2]. Most research has been performed on single cylinder research engines; a limited number of studies have been completed on multi-cylinder research engines [3].

To understand the combustion phenomena inside the cylinder, a model study of a natural gas-diesel dual fuel combustion and emission is performed using the commercial CONVERGE CFD code. A reduced chemical kinetic mechanism with 86 species and 393 reactions for n-heptane, methane, ethane and propane is used. The CONVERGE CFD code, which originates from the KIVA research code software, is selected as the modeling tool for a number of numerical advantages in simulating flows in IC engines. For example, CONVERGE handles the moving boundaries in a completely automatic fashion and the deforming mesh issues typically associated with the moving parts are eliminated. Moreover, the true geometry is maintained during re-gridding. CONVERGE includes advanced numerical techniques and physical models describing processes of spray, turbulence and combustion, and the nonlinear interactions of such processes. These models have been examined and extensively validated in IC engines. In this study, several models are included in order to improve the accuracy of diesel and dual fuel combustion using CONVERGE. The objective of modeling dual fuel combustion is to gain better understanding of the combustion behavior in dual fuel engines. This modeling is performed in conjunction with experimental studies and the simulation results are validated by the experimental data.

ENGINE DESCRIPTION

The engine used is a 6-cylinder Tier II, 6.8 liter turbocharged John Deere 6068H diesel engine with bowl-shaped piston/combustion chamber. It is equipped with a turbocharging system and a high-pressure common rail fuel injection system. The basic specifications are presented in Table-1. The dual fuel system is a retrofit to

the diesel engine. Instead of aspirating only air, natural gas is supplied to the intake upstream of the turbocharger. This allows the air and gas to be mixed by the turbocharger. This premixed charge is then sent through the intercooler and into the intake manifold. No modifications are made to the internal workings of the engine or the injection method of the diesel fuel into the cylinder. The natural gas will displace some of the diesel required to run the engine, decreasing diesel fuel consumption for the same power output. The dual fuel kit has the following major components: Programmable Logic Controller (PLC) - based control panel, supply gas filter, pressure regulator, safety solenoid shut-off valve, and mixer. A full description of experimental apparatus and results is described elsewhere [4, 5, 6, 7].

Table-1. Specifications of the John Deere 6068H.

Bore	106 mm
Stroke	127 mm
Connecting Rod	203 mm
Compression Ratio	17:1
Normal operation speed	1800 rpm
Number of nozzle holes	6
Spray angle	62.5°
Start of injection timing	6.5 bTDC
Rated power	275 hp
Rated speed	2400 rpm
Inlet valve closure	-156.75°

COMPUTATIONAL MODELING

An investigation is performed on diesel and dual fuel combustion and emissions formation using CONVERGE. To reduce computational time, the computational domain is a sector, 1/6 of the cylinder, with periodic boundaries. This sector includes one of the six nozzles of the diesel injector. To further reduce computational time, the compression, combustion, and expansion processes are simulated. The initial properties of residual gas, fuel, and air at intake valve closed (IVC) are specified using information from the experimental observations. The initial pressure, temperature, velocity and turbulence fields at IVC are iterated until it satisfies the motored pressure from experiments (the pressure was within 1%). A set of reduced kinetic mechanisms by Hockett et al. are adopted to further reduce the computational effort [8]. In this study, the gas phase of diesel is modelled as n-heptane because it has a Cetane number close to that of diesel fuel. However, diesel in its liquid state is modelled using the properties of diesel from the CONVERGE library. Natural gas is modelled as a mixture of 85% methane, 10% ethane and 5% propane. The physical properties of the cylinder such as the dimension bore and stroke, injector nozzle diameter, and shape of the piston crown are obtained from John Deere. The Adaptive Mesh Refinement (AMR) is adopted based on temperature and velocity minimum cell size of 0.25mm. Near nozzle region, fixed embedding is used with cell size of 0.25mm. Two cases at low load and high load for each diesel and dual fuel operating mode are modelled.

Spray modeling

In a compression ignition (CI) engine, liquid fuel spray is injected into the combustion chamber near the end of the compression stroke. After injection, the fuel spray undergoes atomization and vaporization processes, followed by fuel-air mixing. Ignition and combustion are integrated in time with those processes. Spray droplets are subject to several processes from the time of blob injection until the time of atomization. Table 2 shows a summary of selected spray models used in this study.The primary breakup process of the liquid fuel is important as it influences downstream processes such as mixing, ignition and combustion. The spray model used in this study is based on the Lagrangian drop Eulerian type. Unless otherwise stated, the characteristics of liquid phase was modeled as a single component acquired from the CONVERGE liquids property library. The blob injection model is used to describe the initial injected droplet size (parent) where it is equal to the nozzle diameter. The hybrid Kelvin-Helmholtz Rayleigh-Taylor (KH-RT) description by Beala and Reitz is used in the droplet breakup model [9]. In this model, the primary atomization (child) process of the initial droplet is due to aerodynamically induced breakup using the KH instability analysis. This primary atomization is also encouraged by aerodynamics in the near-nozzle region and cavitation and turbulence from the injector nozzle. This is modelled using the Kelvin-Helmholtz-Aerodynamics Cavitation Turbulence (KH-ACT) [10]. In addition to the KH breakup mechanism, RT instability is also believed to play an important role in droplet breakup mechanisms. The secondary breakup of these droplets is modelled as a competition between KH and RT mechanisms due to the rapid deceleration of the droplets. As seen in Figure-3, this hybrid KH-RT model allows the RT accelerative instabilities to affect all child droplets and does not use a breakup length to model primary breakup. The droplet collision model is based on No Time Counter (NTC) model by Schmidt and Rutland [11]. This model involves stochastic parcels sub-sampling within a cell, which result in faster and more accurate collision calculations. The spray-wall interaction (liquid drops with solid surfaces model used in this study is a hybrid wall film model. It includes the effect associated with a drop splash based on the Weber number.

Combustion Modeling

The detailed chemistry or SAGE by Senecal is used to model combustion [12]. To solve chemical reactions, SAGE calculates the elementary reaction rate while CFD solves the transport equation. However, to reduce the computational expense, this detailed chemistry is only activated in cells that pass the minimum

temperature and hydrocarbon (HC) mole fraction specified in CONVERGE. In addition, to expedite the detailed chemistry calculations, the multizone chemistry model by Babajimopoulos is also used [13]. The multizone model groups cells that have similar thermodynamic states in zones. In this study, the variables of interest are temperature and reaction ratio. These zones are randomly distributed among different processors to balance the load, therefore reducing computation time.

Turbulence is modeled by the Renormalization Group (RNG) k-ε Reynolds Averaged Navier-Stokes (RANS) model. This RNG k-ε is more robust than the standard k-ε model. The model includes spray compressibility and the effect of turbulence interaction. It provides better predictions for streamline curvature, transitional flows, wall heat and mass transfer. The Turbulence Kinetic Energy (TKE) and Turbulent Dissipation (eps) initial values are provided accordingly. The heat transfer model by Han and Reitz is considered and takes into account the effect of compressible flow [14]. This model is developed from the assumption of one-dimensional energy conservation equation so that the analytical solution of the temperature profile can be obtained.

The shape of the injection rate for accurate combustion modeling is important. However, this information is unavailable; therefore, data is gathered from literature. The rate shape used in this study is based on the injector profile by Andrew et al., which was taken originally from Perini *et al.* [15]. In Perini's study, a set of injection rate shape at different injection pressure is published. Since the amount of the fuel injected and injection durations are different, the rate shape from Andrew *et al*. is modified according to the fuel amount and injection duration used in this study as seen in Figure-1.

Table-2. Key spray processes used in this study using CONVERGE.

Spray model physical process	Models
Liquid injection	Blob injection
Spray breakup	Modified KH-RT
Drop drag	Dynamic drag models
Collision outcomes model	Post
Turbulent Dispersion	O'Rourke model
Drop/wall interaction	No Time Counter (NTC) collision

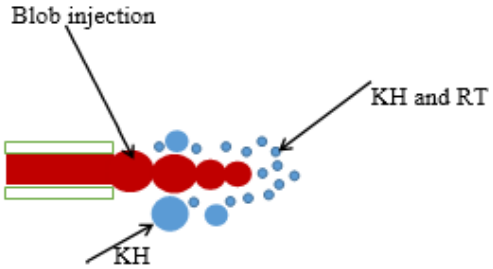

Figure-1. Schematic of the hybrid KH-RT breakup model.

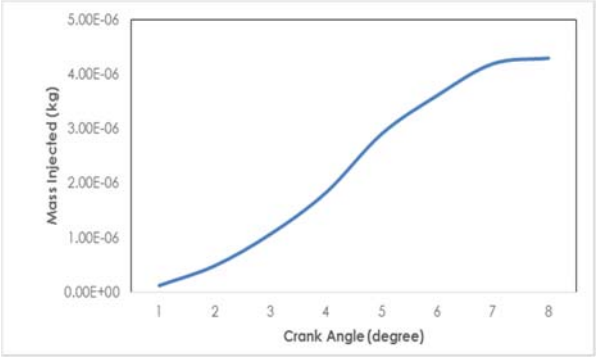

Figure-2. Injector rate shape used in this modelling.

Reduced mechanism

To make efficient calculations, the reduced primary reference fuel mechanism known as CSU86 is used. This reaction mechanism consists of 86 species and 393 reactions for n-heptane, methane, ethane and propane. This reduced mechanism is a combined version of the detailed mechanism from Healy et al. and Yoo *et al* [16]. The detailed methane through n-pentane mechanism consists of 293 species and 1588 reactions. Yoo *et al*. n-heptane mechanism with 88 species is a reduced version from the detailed n-heptane mechanism from Curran et al. with 561 species and 2539 reactions. Detailed description of the CSU86 mechanism is presented by Hockett *et al*. and will not be discussed in detail here. The mass injected is modified according to the injection rate shape and injection duration, as discussed in the previous section.

RESULTS AND DISCUSSIONS

The main objectives of CFD modeling are to understand dual fuel combustion and identify the locations of the formation of emissions in a cylinder. Ultimately, the purpose of this modeling is to prove the hypotheses made in the previous section. Test data is used to demonstrate the validity of the physical models adopted in the CFD simulations. Motored pressure, combustion pressure and net HRR resulted from of the simulations model are compared to the corresponding experimental results. This chapter discusses results from a set of simulation results for the 12% load and the 75% load, focusing on temperature, equivalence ratio and emission distributions in the dual fuel operations. Table-3 and

Table-4 show some of the major values of the dual fuel experiments and modeling at 12% and 75% loads, respectively.

Table-3. A comparison of the main values in a dual fuel experiment and modeling at 12% load.

Parameter	Experiment	Modeling
Start of Injection (°bTDC)	-6.5	-3.0
Injection Duration (°)	Not Measured	9.0
Peak Pressure (kPa)	4464	4379
Diesel Fuel Mass (kg)	1.89e-06	2.8e-06
Temperature at IVC (K)	314.6	398
Pressure at IVC (kPa)	178	92.5

Table-4. A comparison of the main values in a dual fuel experiment and modeling at 75% load.

Parameter	Experiment	Modeling
Start of Injection (°bTDC)	-6.5	-5.5
Injection Duration (°)	Not Measured	10.0
Peak Pressure (kPa)	4382	4290
Diesel Fuel Mass (kg)	3.5e-06	4.5e-06
Temperature at IVC (K)	315	398
Pressure at IVC (kPa)	208	134.8

In-cylinder pressure and heat release rate comparison

The initial pressure is based on the experiment but carefully adjusted and iterated to obtain better results at peak motored pressure. The initial pressure values in Table 3 and Table 4 starts low, but the pressures rise to approach the experimental values. Figure-5 shows the comparison of motored pressure for experiment and simulation at 12% load, indicating that the experimental pressure profile is reproduced and matched in order to carry out the simulations at the same operating conditions. Figure 6 compares the dual fuel experiment and simulation of motored pressure traces at 75% load. As can be seen, the initial pressure in a dual fuel simulation is set a little higher than the experiment to obtain a better peak pressure match.

Figure-7 depicts corresponding pressure variations as a function of crank position in a dual fuel experiment and simulation at 12% load. The dual fuel experiment curve represents an average of more than 100 cycles. While the motored peaks of both traces are matched, the simulation fails to reach a similar peak pressure as the experiment. The simulation pressure rises slightly earlier and falls lower than the experiment. The results show there is an approximately 2% error between simulation and experiment results. The predicted delay period from the simulation follows the experimental data. Figure-8 shows the prediction of in-cylinder pressure with the corresponding data from the experiment at 75% load. The motoring pressure for both cases rise similarly. However, at 4° aTDC the simulation pressure decreases slightly. Then, at 11° aTDC the simulation pressure increases marginally higher than the experiment. This could be due to slightly high diesel mass injection in the simulation. After 17°aTDC, the simulation pressure decreases earlier than experiment pressure. Despite this, the predicted results using the CSU86 mechanism is in good agreement to the experiment.

Figure-9 represents net HRR with a crank position at 12% load. The dual fuel simulation HRR shows slightly later development of combustion at 100 J/degree, while the experiment peaks at less than 80 J/degree. At this load, there is no significant mixing-controlled combustion. HRR continues at a lower rate for both conditions into the expansion stroke. At this point, a small amount of natural gas and n-heptane may have not yet burned as a result of incomplete combustion. Excess fuels end up in the exhaust as HC emission and a product of fuel-rich combustion such as CO.

Figure-10 shows net HRR as a function of a crank angle at 75% load. At this load, both cases show two substantial phases. In diesel combustion, these peaks are identified as premixed and mixing-controlled combustion phases. However, in dual fuel combustion with natural gas as the primary fuel, these combustion phases should be reversed. The first peak is elevated shortly after diesel fuel injection. Since diesel combustion is primarily diffusion flame, therefore the combustion phase is described as mixing-controlled. The second peak rises due to natural gas combustion. Since natural gas is premixed, thus describes the second peak in Figure-10 as premixed combustion phase. In a dual fuel simulation, the heat release rises until it peaks at 170 J/degree. The experiment shows a steady increase of HRR which then peaks at 100 J/degree. After that, it decreases gradually into the lower rate of mixing controlled combustion phase. The more pronounced combustion during the premixedphase may result in high temperature. As seen in Table-4, the injected diesel mass in simulation models is higher than the experiment. In this case, the HRR of the simulation goes beyond the values of the experiment. In dual fuel simulation, the heat release continues at a lower rate into late combustion phase at approximately 20° aTDC while, in dual fuel experiment the late combustion phase occurs at 25°aTDC. At approximately 30° aTDC both operations reach complete combustion.

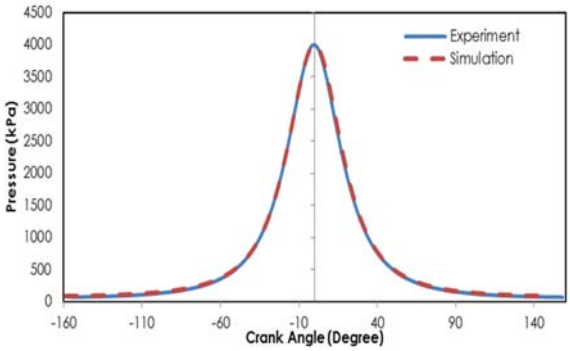

Figure-3. Motored pressure variations as a function of crank angle at 12% load.

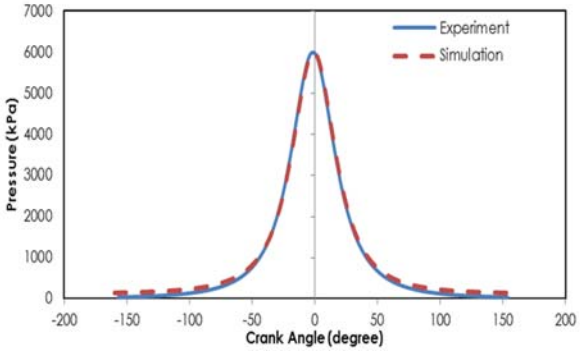

Figure-4. Motored pressure variations as a function of crank angle at 75% load.

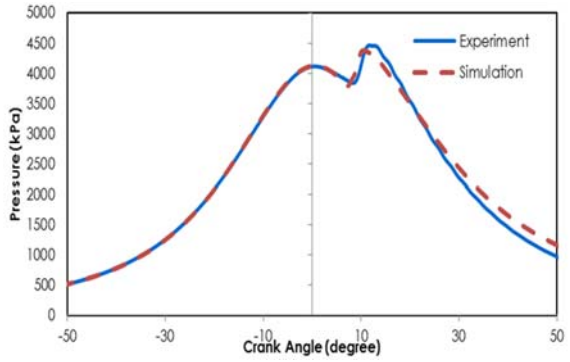

Figure-5. A comparison of pressure traces in a dual fuel experiment and simulation at 12% load.

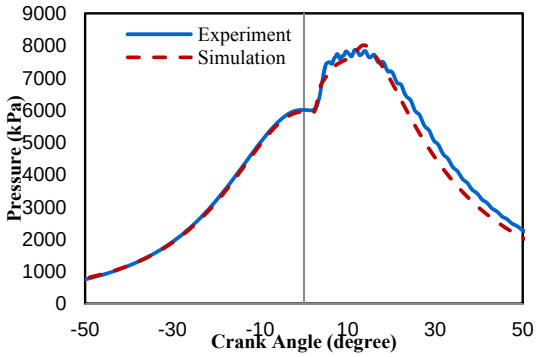

Figure-6. A comparison of pressure traces in a dual fuel experiment and simulation at 75% load.

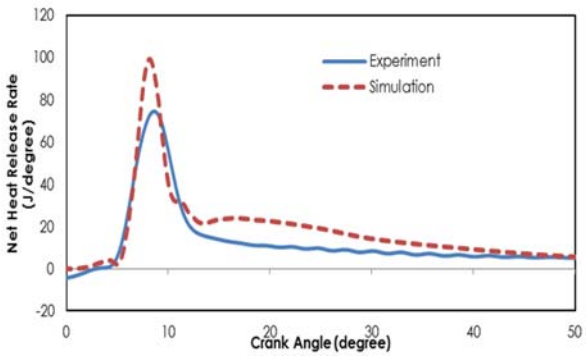

Figure-7. Net HRR for dual fuel experiment and simulation at 12% load.

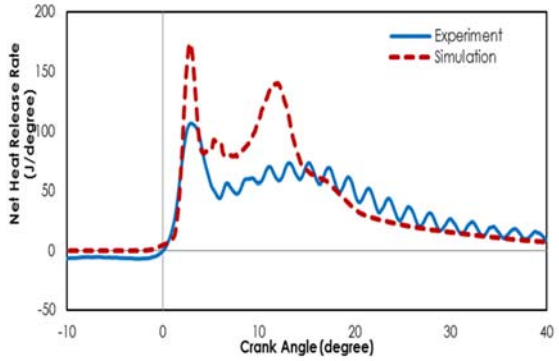

Figure-8. Net HRR for dual fuel experiment and simulation at 75% load.

Temperature Distributions

In this section, only dual fuel simulations at 12% and 75% loads are considered. As mentioned before, the purpose of this modeling study is to conduct an initial guide to better understand natural gas-diesel dual fuel combustion. Therefore, temperature contours and equivalence ratio in dual fuel simulations at 12% and 75% loads are presented and discussed here.

The temperature distributions in dual fuel engines at various crank positions are predicted using CONVERGE code as shown in Figure-9.

The temperature profile is sliced through the spray axis. The temperature distribution at 12% load is presented on the left column, while the right column represents the distribution at 75% load. The green contours represent natural gas flame or premixed while diesel flames or non-premixed is illustrated by the red contours. The data presented here is at odd crank starting at 5° until 27° aTDC. The 5° is chosen due to the significant temperature profile and emissions formation that occur in this stage. At crank angle of 27°aTDC, most dissociated product gases that appear at this crank position are assumed to exist in the exhaust as emissions.

The general flame structure in each load remains similar during the crank positions i.e. a flame is initially grow rapidly as a result of diesel fuel ignition and non-premixed combustion, then slows down as a result of natural gas premixed combustion. Comparing both loads at all crank positions, higher temperature flames are observed in 75% load than in 12% load. At 75% load, more diesel fuel mass is injected, therefore more volume charge is affected by diesel fuel combustion increasing the burning of natural gas and air mixture. At 12% load in contrast, many low temperature regions (blue contours) are observed as a result of incomplete combustion and fuel-rich combustion. Lower temperatures are expected in 12% load operation due to a leaner mixture and a smaller amount of diesel injected. This phenomenon is supported by lower net HRR at 12% load compared to 75% load, as shown in Figure-9 and Figure-10. At the end of the combustion at 27° aTDC, many regions are still unburned leading to higher HC and carbon monoxide emissions in 12% load.

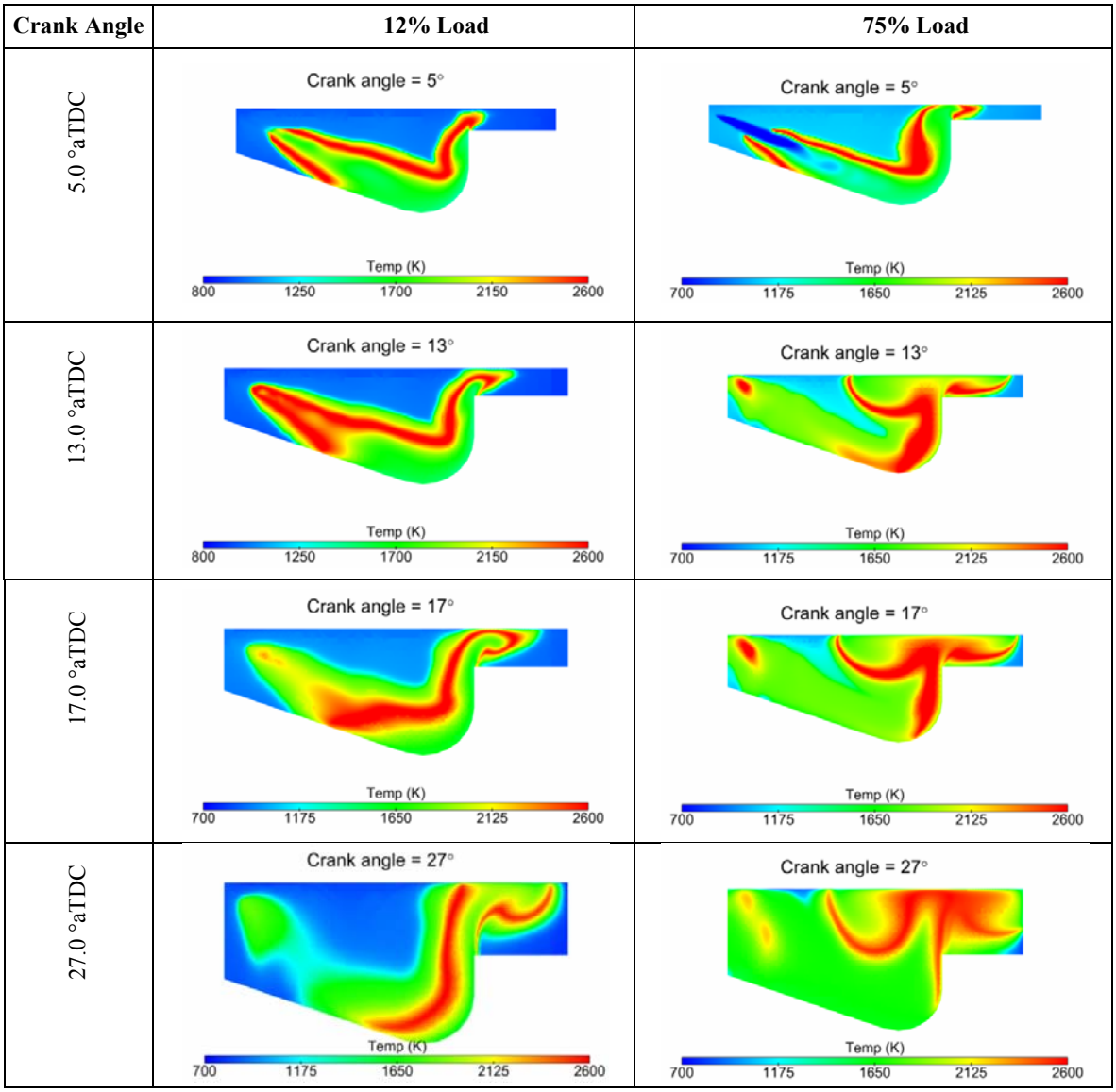

Figure-9. A set of temperature profiles at various crank angles at 12% and 75% loads.

Equivalence ratio distributions

Equivalence ratio is an important parameter that describes the formation of emissions inside the cylinder. HC, CO and oxides of nitrogen (NO_x) emissions are affected by equivalence ratio. As the mixture goes richer, there is not enough oxygen to react with all the carbon and hydrogen, thus resulting in higher HC and CO emissions. HC is also high in very lean mixtures due to misfire and poor combustion. Peak NO_x is formed at equivalence ratio = 0.95, which is a slightly leaner mixture. At this stage, the combustion temperature is high and not all oxygen reacts with nitrogen. Figure-10 shows equivalence ratio distributions across the cylinder at crank angle 5° to 29° aTDC at 12% and 75% loads. In Figure-10, the rich region behavior is presented by red and green contours. It is clearly shown that the locations of rich region are different between the two cases. In 12% load, the rich region is identified mostly at piston bowl wall and near the clearance height wall. While, in 75% load the rich regions are located mostly at cylinder head. The equivalence ratio trend follows the diesel temperature flame propagations. For this reason, it is expected that the formations of HC and CO are high in these regions.

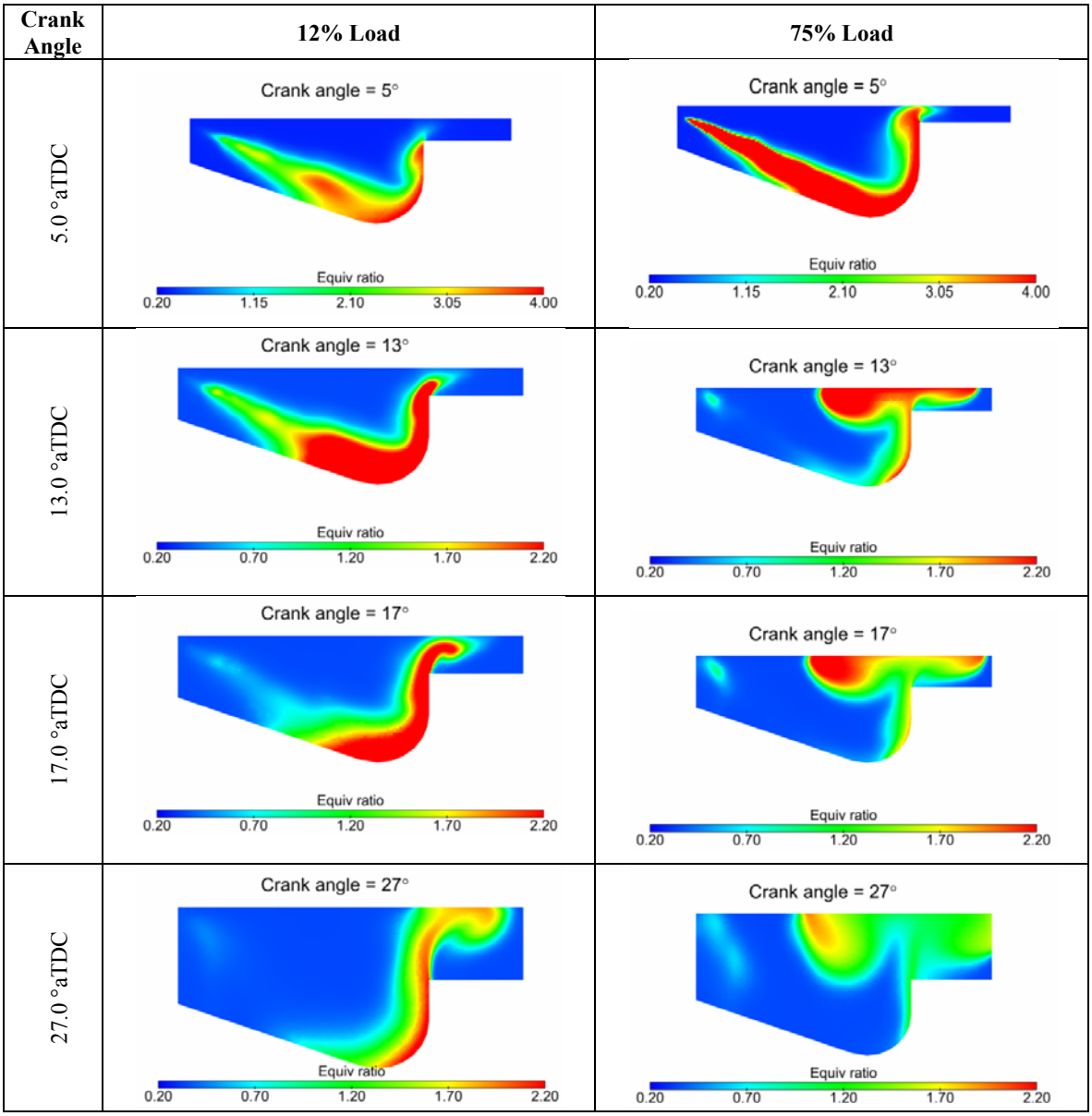

Figure-10. A set of temperature profiles at various crank angles at 12% and 75% loads.

Carbon Monoxides Distributions

The variations of CO emissions at various crank angles for 12% and 75% loads are presented in Figure-11. At 12% load, the formation of CO is mainly located near the piston bowl wall. At 75% load, CO emission is observed mostly at cylinder head. As presented in Figure-11, the locations of high CO is observed at high Φ, which explains the direct relationship of Φ and CO formation.

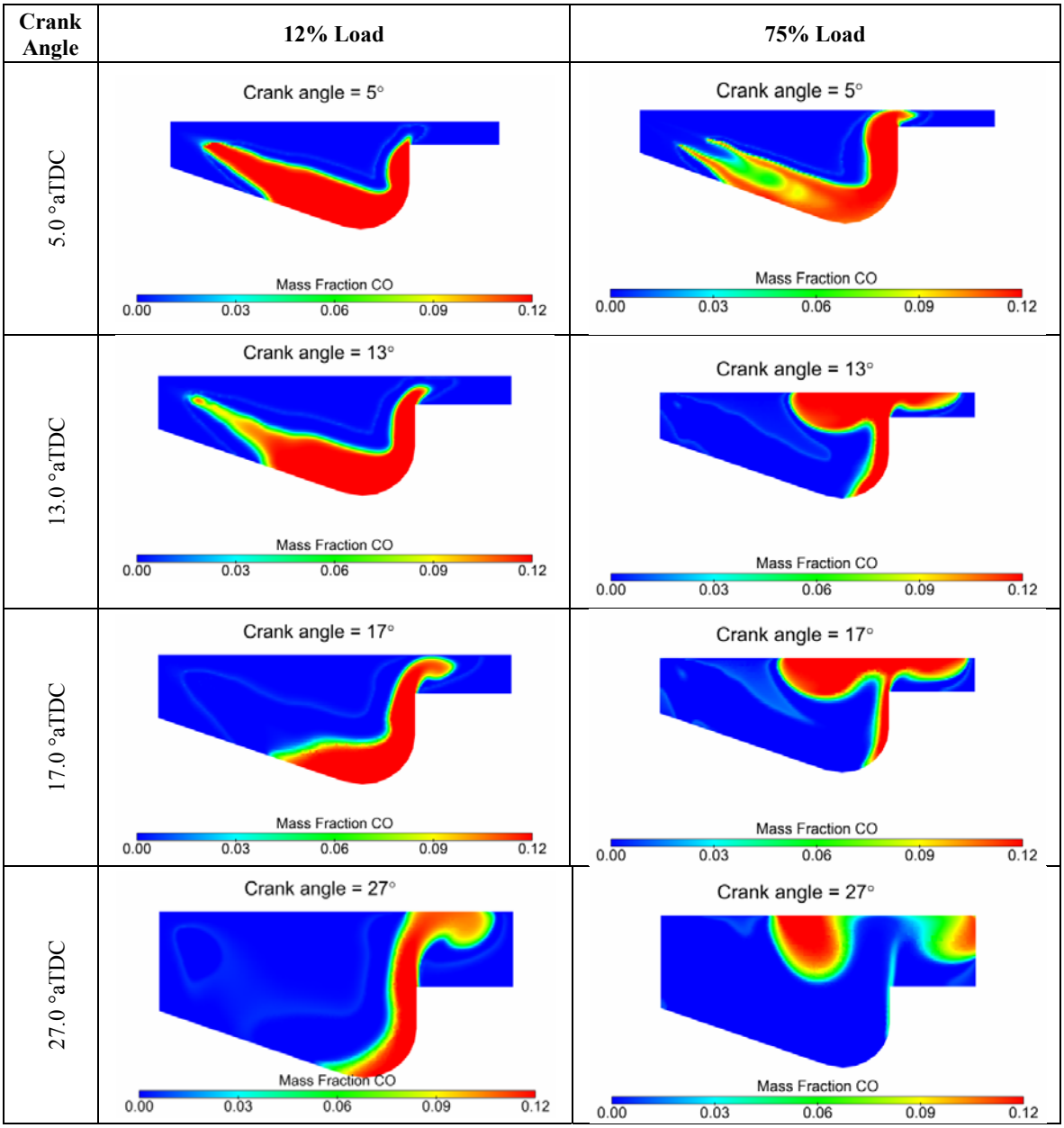

Figure-11. A set of CO distributions at various crank angles at 12% and 75% loads.

Hydrocarbons distributions

HC emissions are presented by unburned CH4 fuel during the combustion process. Figure-12 shows the contours of CH4 mass fraction for 12% and 75% load at various crank angle degrees. The view from on top of the Z- and spray axis is presented to illustrate HC emissions in a cylinder. At a crank position of 9° aTDC, a high amount of CH4 is burned at 75% load, while some are left unburned near the cylinder and piston head. Compared to the 12% load, most of CH4 is unburned during the combustion process at nozzle area, piston and cylinder head. Towards the end of the combustion phase at 27° aTDC, a very small amount of HC is observed in the 75% load while a large amount of CH4 mass fraction is still unburned. At 75% load, two plane sections are shown to illustrate the location of HC emissions.

From the figure, it shows that the formation of HC in dual fuel combustion occurs due to the leaner

mixture, and not the rich mixture. The effect is substantial in 12% load where the mixture is below the flammability limits. At 75% load, more diesel is injected even though the mixture is lean, thus promoting the combustion of the natural gas and air mixture.

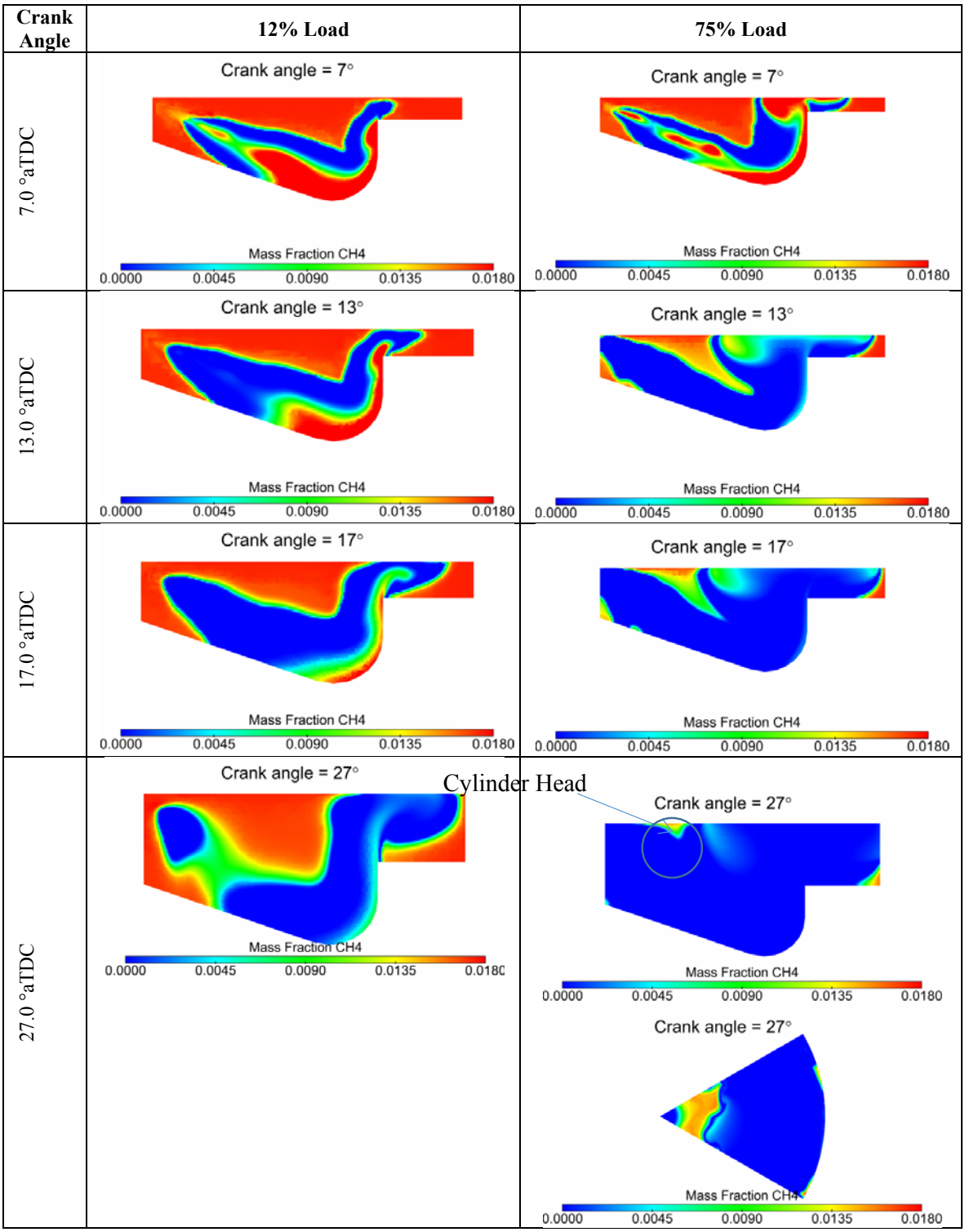

Figure-12. Predicted HC emissions as CH4 mass fraction across the cylinder at 12% and 75% loads.

CONCLUSIONS

A modeling study of a natural gas-diesel dual fuel combustion and emission is performed using the commercial CONVERGE CFD code. A reduced chemical kinetic mechanism with 86 species and 393 reactions for n-heptane, methane, ethane and propane is used. Conclusions for the investigation into dual fuel combustion using CONVERGE and CSU86 reduced mechanism in conjunction with experiment at 12% and 75% loads are as follows:

a) Overall, the peak pressure in dual fuel simulation is slightly higher than dual fuel experiment. The HRR is over predicted compared to the experiments. The post-processed data illustrates the premixed and non-premixed flame temperature in dual fuel engine.
b) Findings showed that CO formation in 12% load of dual fuel engine is mainly located at the piston bowl rim. While in 75% load, the formation of CO is observed mostly at cylinder head.
c) At low load, HC emission is observed higher than at high load especially around the injector. From the simulation results, it is revealed that HC formation in dual fuel operation occurs due to lean mixture of natural gas and air.
d) CSU86 reduced mechanism is a reliable mechanism for predicting the natural gas and diesel combustion in dual fuel engine.

REFERENCES

[1] Papagiannakis R.G., Rakopoulos C.D., Hountalas D.T. and Rakopoulos D.C. 2010. Emission characteristics of high speed, dual fuel, compression ignition engine operating in a wide range of natural gas/diesel fuel proportions. Fuel. 89: 1397-1406.

[2] Papagiannakis R.G. and Hountalas D.T. 2003. Experimental investigation concerning the effect of natural gas percentage on performance and emissions of a DI dual fuel diesel engine. Applied Thermal Engineering. 23: 353-365.

[3] Sahoo B.B., Sahoo N. and Saha U.K.2009. Effect of engine parameters and type of gaseous fuel on the performance of dual-fuel gas diesel engines- a critical review. Renewable and Sustainable Energy Reviews. 13: 1151-1184.

[4] Wan Nurdiyana W.M., Jennifer V. and Daniel O. 2015. Effects of diesel displacement on the emissions characteristics of a diesel derivative dual fuel engine. ARPN Journal of Engineering and Applied Sciences. 10: 9553-9561.

[5] W. N. Wan Mansor, J. S. Vaughn and D.B. Olsen. 2014. Emissions and efficiency evaluations of a 6.8 liter diesel derivative dual fuel engine. Proceedings of the Canadian Society for Mechanical Engineering International Congress.

[6] Wan Nurdiyana Wan Mansor. 2014. Dual fuel engine combustion and emissions - an experimental investigation coupled with computer simulation. Ph.D. Dissertation, Colorado State University, Fort Collins, CO.

[7] Wan Nurdiyana Wan Mansor, Jennifer S. Vaughn, Daniel B. Olsen. 2014. Experimental evaluation of diesel and dual fuel combustion in a 6.8 liter compression ignition engine. 2014 Spring Technical Meeting Western States Sections of the Combustion Institute.

[8] Hockett A. 205. A Computational and Experimental Study on Combustion Processes in Natural Gas/Diesel Dual Fuel Engines. Ph.D. Dissertation, Colorado State University, Fort Collins, CO.

[9] Beale J. and Reitz R. 1999. Modeling Spray Atomization with the Kelvin-Helmholtz/Rayleigh-Taylor Hybrid Model. Atomization and Sprays. 9: 623-650.

[10] Som S. and Aggarwal, S. K.2010. Effect of primary breakup modeling on spray and combustion characteristics of compression ignition engines. Combustion and Flame.pp. 1179-1193.

[11] Schmidt D. P. and Rutland C. J. 2000. A New Droplet Collision Algorithm. J. Comp. Phys.p. 62.

[12] Senecal P.K., Pomraning E. and Richards K.J. 2003. Multi-Dimensional Modeling of Direct-Injection Spray Liquid Length and Flame Lift-off Lenght using CFD and Parallel Detailed Chemistry. SAE Paper.

[13] Babajimopoulos A. *et al*. 2005. A coupled computational fluid dynamics and multi-zone model with detailed chemical kinetics for the simulation of premixed charge compression ignition engines. International Journal of Engine Research. p. 49.

[14] Han Z. and Reitz R.D.1997. A Temperature Wall Function Formulation for Variable Density Turbulence Flow with Application to Engine Convective Heat Transfer Modeling. Int. J. Heat and Mass Transfer.

[15] Perini F. *et al*.2013. A Computational Investigation of the Effects of Swirl Ratio and Injection Pressure on

Mixture Preparation and Wall Heat Transfer in a Light-Duty Diesel Engine. SAE Technical Paper, 1.

[16] Healy D., *et al*. 2010 Oxidation of C1-C5 Alkane Quinternary Natural Gas Mixtures at High Pressures. Energy and Fuels. pp. 1521-1528.